Available online at www.sciencedirect.com
ScienceDirect
Physics Procedia 3 (2010) 659–665
Physics Procedia
www.elsevier.com/locate/procedia

International Congress on Ultrasonics, Universidad de Santiago de Chile, January 2009

High Resolution Ultrasound Imaging Using Adaptive Beamforming with Reduced Number of Active Elements

Iben Kraglund Holfort[a] *, Fredrik Gran[b] and Jørgen Arendt Jensen[a]

[a]*Technical University of Denmark, Dept. Electrical Engineering, Center for Fast Ultrasound Imaging, DK-2800 Kgs. Lyngby, Denmark*
[b]*GN ReSound A/S, Lautrupvej 7, DK-2750 Ballerup, Denmark*

Abstract

In this paper, the adaptive, minimum variance (MV) beamformer is applied to ultrasound data. Due to near-field properties, the energy of the ultrasound data reduces towards the edges of the transducer. The influence of this near-field effect is demonstrated, and a method to reduce this influence is proposed. By reducing the number of active sensor elements, an increased resolution can be obtained with the MV beamformer. This observation is directly opposite the well-known relation between the spatial extent of the aperture and the achievable resolution. The investigations are based on Field II simulated data using a 128-element transducer with a large spatial extent. The results show that an increased resolution can be obtained, when using only the central part of the transducer compared to using the entire spatial extent. Using the central 32 or 48 elements provides an increased resolution compared to using all 128 elements.

Keywords: Adaptive Array Processing; Adaptive Beamforming; High Resolution Beamforming; Minimum Variance Beamforming; Ultrasound Imaging

1. Introduction

In medical ultrasound imaging, beamforming is conventionally carried out using the Delay and Sum (DS) beamformer, which works by delaying, weighting and summing the individual sensor signals. The DS beamformer uses pre-defined and fixed apodization weights. It is a well-known fact that the achievable resolution is directly dependent on the choice of apodization weights and the number of sensor elements.

Within recent years, the application of adaptive beamforming to ultrasound imaging has become an area of increasing interest. The primary focus has been on the so-called Minimum Variance (MV) or Capon beamformer [1]. Despite the fact that adaptive beamformers originally were developed for far-field applications, previous

* Corresponding author. Tel.: +45 4525 3705; fax: +45 4588 0117.
E-mail address: ikh@elektro.dtu.dk

doi:10.1016/j.phpro.2010.01.083

investigations in the field of ultrasound imaging have shown promising results; in terms of significantly increased resolution [2]-[8].

Due to near-field properties, the energy of the ultrasound data reduces towards the edges of the transducer. In this paper, the influence of this near-field effect on the MV beamformer is demonstrated using simulated Field II [9]-[10] data. Furthermore, a method to reduce this influence is proposed by reducing the number of sensor signals.

2. Adaptive Beamforming

A beamformer works by delaying, weighting and subsequently summing each of the sensor signals. As illustrated in Fig. 1, an adaptive beamformer is similar to DS with the only difference being the choice of weights. The adaptive weights are continuously updated and are directly dependent on the measured sensor signals.

2.1. Pre-steering

As in conventional beamforming, the sensor signals are pre-steered at the focus point, so that the sensor responses from the focus point will sum in phase, and the DS beamformer output from the current point will be maximized. Pre-steering at a point is carried out by compensating for the propagation delay for this point. The delay is calculated as the propagation path from the transmit element to the focus point and back to the receiving element.

The concept of pre-steering is illustrated in Fig. 2(a)-(b), which show the responses from three point targets located at (x,z)={(0,40), (5,42), (-2,45)} mm. The responses are simulated for a transducer with 128 elements. Fig. 2(a) shows the received sensor signals, and in Fig. 2(b), the sensor signals are pre-steered at the point (x,z)= (0,40) mm. Due to the compensation for the delay, the response from the focus point resembles a plane wave impinging directly onto the array. Thus, the signals will sum in phase, and the DS beamformer output will be maximized. This plane wave resemblance is exploited in the adaptive beamformer, see Sec. B.3.

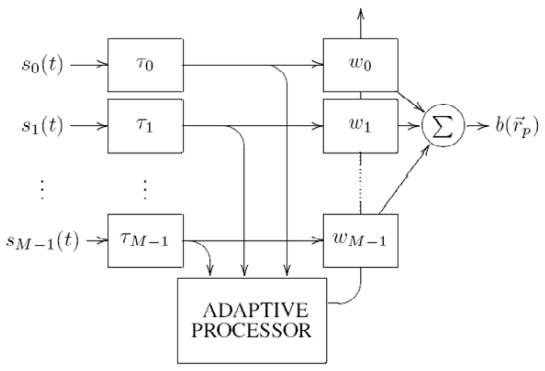

Fig.1 Block diagram of an adaptive, narrowband beamformer. The adaptive processor determines a set of optimized apodization weights from the delayed sensor signals.

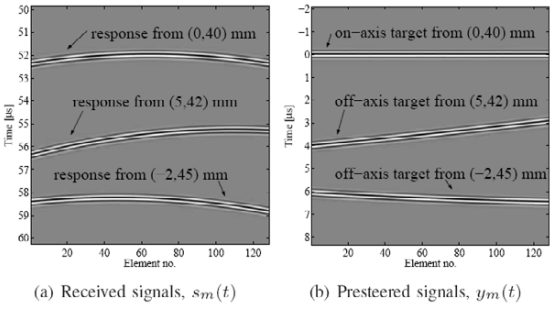

(a) Received signals, $s_m(t)$ (b) Presteered signals, $y_m(t)$

Fig.2 (a) The received sensor signals. The figure shows the responses from three point targets located at (x,z) = {(0,40),(5,42),(-2,45)} mm. (b) Sensor signals pre-steered at the focus point (x,z) = (0,40) mm. After pre-steering, the response from the focus point resembles a plane wave impinging directly onto the array.

2.2. Beamforming

Denoting the *m*th pre-steered sensor signals $y_m(t)$, the beamformer output is given as a weighted sum of the sensor signals

$$b(r) = \sum_{m=0}^{M-1} w_m y_m(0) = w^H y \tag{1}$$

where r denotes the current focus point and the superscript $\{\}^H$ denotes the Hermitian transpose. Using pre-defined and fixed apodization weights, w_m, yields the DS response.

2.3. Minimum Variance Beamforming

In adaptive beamforming, the apodization weights are varying and are directly dependent on the sensor signals. The Minimum Variance (MV) beamformer continuously updates the weights, so that the variance (or power) of the beamformer output is minimized, while the response from the focus point is passed without distortion. Mathematically, this is expressed as [1]

$$min\, w^H R w \;\; subject\ to \;\; w^H e = 1 \tag{2}$$

where R is the covariance matrix of the pre-steered sensor signals, and e is the so-called steering vector. The steering vector characterizes the signal of interest, which is not to be distorted.

The constrained optimization problem (2) can be solved analytically using Lagrangian multiplier theory. Provided that R^{-1} exists, the MV optimized apodization weights are given by [1]

$$\hat{w} = \frac{R^{-1} e}{e^H R^{-1} e} \tag{3}$$

2.3.1. Covariance Matrix Estimation

The covariance matrix is unknown and must be replaced by the sample covariance matrix, which is estimated from the data. To estimate the sample covariance matrix a number of realizations of data is required. In this paper, these realizations are obtained by dividing the data from a single acquisition into a number of groups. This follows the spatial smoothing approach suggested in [11].

As illustrated in Fig. 3, the spatially smoothed covariance matrix estimate is obtained by dividing the array into P overlapping sub-arrays. For each sub-array, a sub-covariance matrix is estimated, and these are averaged across the array. Note that this reduces the dimension of the covariance matrix, and thus the number of weights will be reduced correspondingly. The reduced dimension also influences the resolution due to the inherent compromise between the width of the array and the achievable resolution [12].

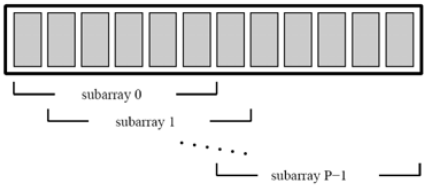

Fig.3 Spatial smoothing. The array is divided into P overlapping sub-arrays, and the covariance matrix is averaged across the array.

2.3.2. Signal of Interest

As indicated in (2)-(3), the definition of the signal of interest, *e*, is of great influence on the MV beamformer output. This signal of interest characterizes the signal emerging from the focus point. As seen in Fig. 2(b) the signal from the focus point will resemble a plane wave, where all sensor signals are in phase, impinging directly onto the array. Thus, standard procedure is to denote the pre-steered signal of interest by a vector of ones, which indicates a constant phase and constant amplitude across the array.

However, in near-field situations, the amplitude is not necessarily constant across the array. Fig. 4-5 show the received sensor signals for a point positioned at (0,50) mm using two 128-element transducers with different spatial extents; a transducer with 0.15 μm pitch (Fig. 4) and 0.3 μm pitch (Fig. 5). For the small transducer, the plane wave resemblance nearly holds. However, for the large transducer, the amplitude drops significantly towards the edges of the transducer; and the constant amplitude plane wave assumption does not hold. Thus, the signal emerging from the focus point will not be passed without distortion as intended. And as seen in the following section, the amplitude difference across the array influences the achievable resolution.

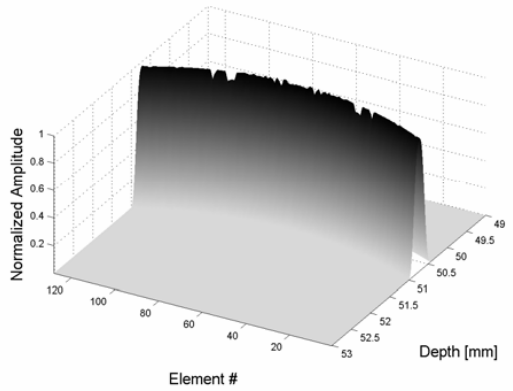

Fig.4 Received sensor signals for a point positioned at (0,50) mm using a 128-element transducer with 0.15 μm pitch.

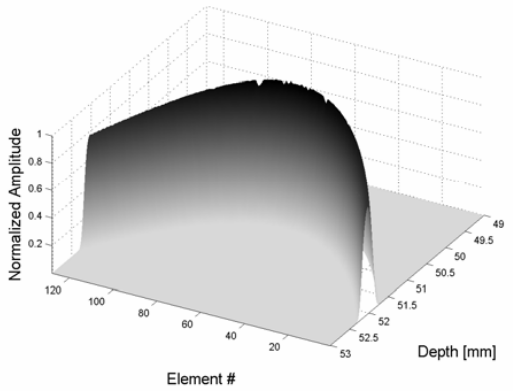

Fig.5 Received sensor signals for a point positioned at (0,50) mm using a 128-element transducer with 0.3 μm pitch.

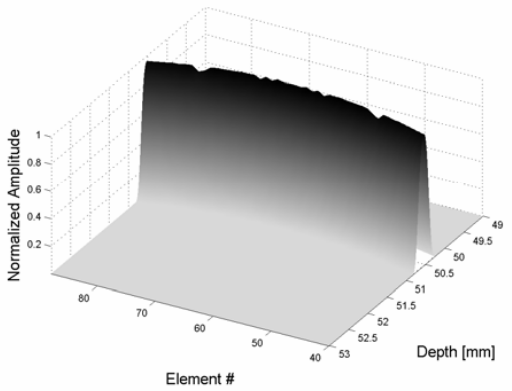

Fig.6 Received sensor signals for a point positioned at (0,50) mm using a 128-element transducer with 0.3 μm pitch. Only the center 48 elements are displayed.

There are several approaches to reduce the influence of the amplitude drop; e.g. changing the analytical expression of the signal of interest, normalizing the amplitudes across the array or virtually reducing the spatial extent of the transducer by reducing the number of active elements. Instead of using all 128 elements, we will only use e.g. the center 48 element, as shown in Fig. 6. The transducer parameters used to create Fig. 5-6 are exactly identical; the only difference is the number of elements used to display the sensor signals. It is seen that the amplitude difference across the array has decreased significantly, and the plane wave assumption now holds.

The majority of the transducers available in our lab has relatively large spatial extents and provides sensor signals with amplitude differences across the array. Thus, a reduction of this influence is of great interest for our future work in this area.

In this paper, we propose an approach using a reduced number of sensor signals to form the adaptive beamformer output. The following section will demonstrate that it is possible to obtain an increased resolution, despite a decreased number of active sensor signals. Note that this principle is directly contradicting the well-known relationship between the number of elements and the achievable resolution.

3. Results

In this section the MV beamformer is applied to Field II [9]-[10] simulated ultrasound data. For the simulations, a 128-element, 5.5 MHz linear array transducer with 0.3 μm pitch is used. These parameters correspond to a transducer, which is physically present in our lab. Data is obtained using a synthetic aperture approach [13], where 11 elements are used as the transmitting aperture and all elements are used as the receiving aperture.

The MV beamformer is implemented in the frequency domain using the short-time Fourier transform with a segment size corresponding to the length of the excitation pulse convolved with the two-way impulse response of the transducer. This provides a set of adapted apodization weights for each frequency bin. Before beamforming white Gaussian noise is added to each of the sensor signals; and a sub-array size of $L=16$ is used for all calculations.

The beamformed responses in this section corresponds to a single synthetic aperture emission, and data are obtained for two point targets positioned at (2,50) mm and (-2,50) mm. Different number of active elements are used; corresponding to {128, 64, 48, 32} elements. This means that the spatial extent of the aperture has been reduced virtually down to 75% of the full size.

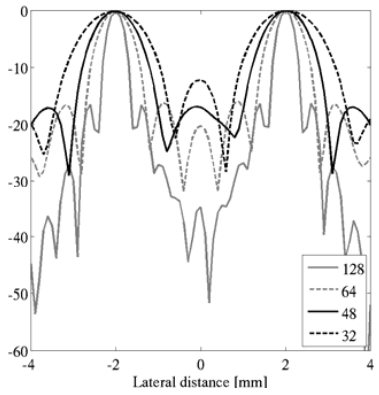

Fig.7 DS beamformed responses with Boxcar weights for two points positioned at (-2,50) mm and (2,50) mm. Different number of active elements, {128, 64, 48, 32} are used.

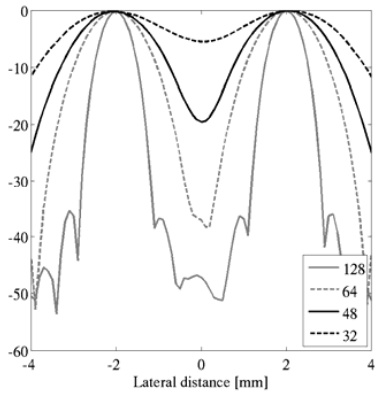

Fig.8 DS beamformed responses with Hanning weights for two points positioned at (-2,50) mm and (2,50) mm. Different number of active elements, {128, 64, 48, 32} are used.

Fig. 7 shows the DS beamformed responses with Boxcar weights. As expected the responses using the highest number of elements provide the highest resolution and contrast; in terms of narrow main-lobe and low side-lobes. And obviously, the DS beamformed responses with Hanning weights, Fig. 8, show exactly the same.

The MV beamformed responses are shown in Fig. 9. It is seen that the MV beamformer provides an increased resolution compared to the responses in Fig. 7-8. Furthermore, it is seen that the highest resolution is not obtained using the largest number of active elements. It is seen that the broadest main-lobe is obtained using 128 elements; and the fewer active elements, the more narrow the main-lobe becomes. Obviously, the number of active elements has a lower bound, and a inherent compromise between the number of active elements and the achievable resolution and contrast exists. The optimum compromise is dependent on the *f*-number, the transducer parameters, and the size of the sub-array for the covariance matrix estimation.

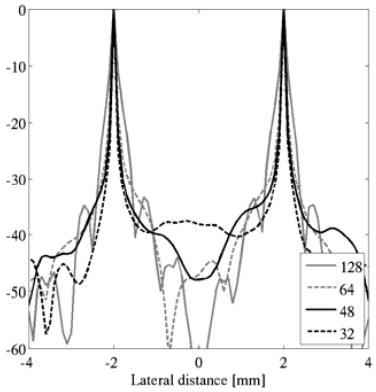

Fig.9 MV beamformed responses for two points positioned at (-2,50) mm and (2,50) mm. Different number of active elements {128, 64, 48, 32} are used.

The purpose of this paper is to illustrate this rather peculiar observation, which is strictly contradicting both the expectation and is directly opposite the observation of the DS beamformer in Fig. 7-8.

4. Conclusions

From the investigations in this paper it is concluded that the near-field effects of ultrasound data has influence on the achievable resolution of the MV beamformer. An approach to reduce the influence of this effect has been proposed using fewer receiving elements. This observation is strictly opposite the expectation.

Acknowledgment

This work was supported by grant 26-04-0024 from the Danish Science Foundation and by B-K Medical ApS, Denmark.

References

[1] J. Capon, “High-Resolution Frequency-Wavenumber Spectrum Analysis,” Proc. IEEE, vol. 57, no. 8, pp. 1408–1418, August 1969.
[2] I. K. Holfort, F. Gran, and J. A. Jensen, “Minimum Variance Beamforming for High Frame-Rate Ultrasound Imaging,” in Proc. IEEE Ultrason. Symp., Oct. 2007, pp. 1541–1544.
[3] I. K. Holfort, F. Gran, and J. A. Jensen, “Plane Wave Medical Ultrasound Imaging using Adaptive Beamforming,” in Proc. 5th IEEE Sensor Array and Multichannel Signal Proc., July 2008, pp. 288-292.
[4] I. K. Holfort, F. Gran, and J. A. Jensen, “Investigations of Sound Speed Errors in Adaptive Beamforming,” in Proc. IEEE Ultrason. Symp., Nov. 2008.
[5] M. Sasso and C. Cohen-Bacrie, “Medical Ultrasound Imaging Using the Fully Adaptive Beamformer,” in Proc. IEEE Int. Conf. Acous., Speech, Sig. Pro., March 2005, vol. 2, pp. 489–492.
[6] F. Viola and W. F. Walker, “Adaptive Signal Processing in Medical Ultrasound Beamforming,” in Proc. IEEE Ultrason. Symp., 2005, vol. 4, pp. 1980–1983.
[7] J.-F. Synnevåg, A. Austeng, and S. Holm, “Adaptive Beamforming Applied to Medical Ultrasound Imaging,” IEEE Trans. Ultrason., Ferroelec., Freq. Contr., vol. 54, no. 8, pp. 1606–1613, Aug. 2007.
[8] Z. Wang, J. Li, and R. Wu, “Time-Delay- and Time-Reversal-Based Robust Capon Beamformers for Ultrasound Imaging,” IEEE Trans. Med. Imag., vol. 24, no. 10, pp. 130–1322, Oct. 2007.
[9] J. A. Jensen and N. B. Svendsen, “Calculation of pressure fields from arbitrarily shaped, apodized, and excited ultrasound transducers,” IEEE Trans. Ultrason., Ferroelec., Freq. Contr., vol. 39, pp. 262–267, 1992.
[10] J. A. Jensen, “Field: A program for simulating ultrasound systems,” Med. Biol. Eng. Comp., vol. 10th Nordic-Baltic Conference on Biomedical Imaging, Vol. 4, Supplement 1, Part 1, pp. 351–353, 1996b.
[11] T.-J. Shan and T. Kailath, “Adaptive Beamforming for Coherent Signals and Interference,” IEEE Trans. Acous., Speech, Sig. Pro., vol. 33, no. 3, pp. 527–536, June 1985.
[12] D. H. Johnson and D. E. Dudgeon, Array Signal Processing. Concepts and Techniques., Prentice-Hall., Englewood Cliffs, New Jersey, 1993.
[13] S. I. Nikolov and J. A. Jensen, “In-vivo synthetic aperture flow imaging in medical ultrasound,” IEEE Trans. Ultrason., Ferroelec., Freq. Contr., vol. 50, no. 7, pp. 848–856, 2003.